Diameter Modulation of Vertically Aligned Single-Walled Carbon Nanotubes

Rong Xiang,[†,*] Erik Einarsson,[‡,§] Yoichi Murakami,[⊥] Junichiro Shiomi,[‡] Shohei Chiashi,[‡] Zikang Tang,[†,∥] and Shigeo Maruyama[‡,*]

[†]State Key Laboratory of Optoelectronic Materials and Technologies, School of Physics and Engineering, Sun Yat-Sen University, Guangzhou 510275, China, [‡]Department of Mechanical Engineering and [§]Global Center of Excellence for Mechanical Systems Innovation, The University of Tokyo, 7-3-1 Hongo, Bunkyo-ku, Tokyo 113-8656, Japan, [⊥]Global Edge Institute, Tokyo Institute of Technology, 2-12-1 Ookayama, Meguro-ku, Tokyo 152-8550, Japan, and [∥]Department of Physics, Hong Kong University of Science and Technology, Clear Water Bay, Hong Kong, China

ABSTRACT

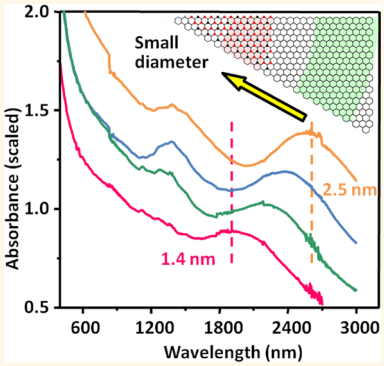

We demonstrate wide-range diameter modulation of vertically aligned single-walled carbon nanotubes (SWNTs) using a wet chemistry prepared catalyst. In order to ensure compatibility to electronic applications, the current minimum mean diameter of 2 nm for vertically aligned SWNTs is challenged. The mean diameter is decreased to about 1.4 nm by reducing Co catalyst concentrations to 1/100 or by increasing Mo catalyst concentrations by five times. We also propose a novel spectral analysis method that allows one to distinguish absorbance contributions from the upper, middle, and lower parts of a nanotube array. We use this method to quantitatively characterize the slight diameter change observed along the array height. On the basis of further investigation of the array and catalyst particles, we conclude that catalyst aggregation—rather than Ostwald ripening—dominates the growth of metal particles.

KEYWORDS: single-walled carbon nanotube · vertical alignment · diameter control · catalyst aggregation

Controlling the size of a nanomaterial is critical for its application because the characteristic length of a material significantly affects its mechanical, thermal, chemical, and particularly electronic properties. This well-known "size effect" has been intensively demonstrated in a variety of systems, including quantum dots, nanotubes, nanowires, nanoribbons/belts, *etc.*[1−3] For a single-walled carbon nanotube (SWNT), the diameter primarily determines the band gap of a semiconducting nanotube and is therefore directly related to the performance of this material in electronics and optics applications.[4,5]

In 2004, we reported the first vertically aligned (VA) SWNT array,[6] which was synthesized by alcohol catalytic CVD (ACCVD). This method yields high-quality SWNTs with an average diameter of 2 nm. Since then, there have been considerable attempts to control the diameter of VA-SWNTs, among which the most successful work was reported in 2006 by Yamada *et al.*, who managed to continuously tune the average diameter of the SWNTs from 2 to 5 nm.[7] More recently, Hart *et al.* demonstrated successful control over the diameter as well as the number of walls for single-walled and few-walled carbon nanotubes (CNTs), being able to adjust the diameter from 5 to 100 nm.[8] However, extension of the range of VA-SWNT diameters to less than 2 nm remains a critical challenge. Earlier this year, Zhong *et al.* proposed a three-layer AlO_x/Fe/AlO_x catalyst−support design that could produce sub-2 nm VA-SWNTs. The dense VA-SWNTs obtained in that work show a great promise for the use of SWNTs as interconnects.[9] More generally, because the band gap is roughly inversely proportional to the diameter, smaller diameter SWNTs are of interest for most electronics and optics applications.

The absence of small-diameter VA-SWNTs is mainly because the catalyst particles used for synthesizing VA-SWNTs are normally prepared by sputtering or evaporation.[10−13] In these conventional physical vapor deposition methods, it is an intrinsic challenge to reduce the size of the metal catalyst particles, which determine the size of the grown SWNT,[14] while maintaining sufficient density necessary for vertical alignment. Here we report the ability to produce VA-SWNT

* Address correspondence to xiangr2@mail.sysu.edu.cn, maruyama@photon.t.u-tokyo.ac.jp.

Received for review June 21, 2012 and accepted July 19, 2012.

Published online July 19, 2012
10.1021/nn302750x

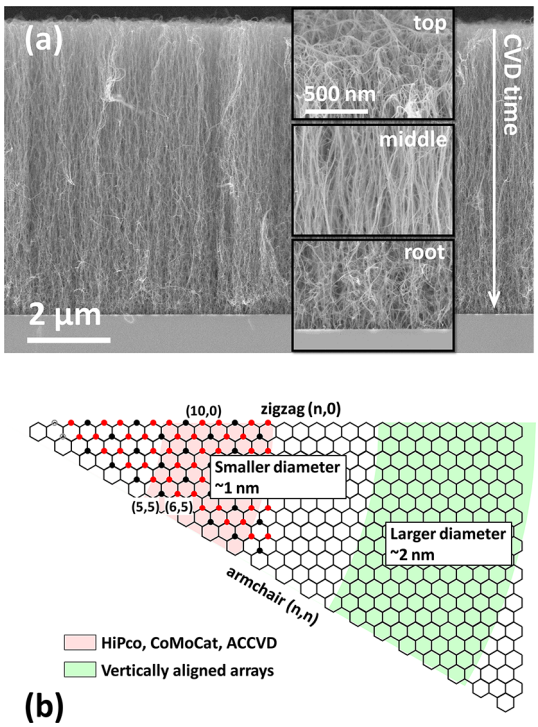

Figure 1. (a) Typical SEM image of a vertically aligned SWNT array grown on a quartz substrate shows the worsening alignment from top to bottom; insets are enlarged images of the top, middle, and root of the array. The scale bar applies to all three images. (b) Graphene lattice showing the chirality range of typical randomly aligned SWNTs (indicated in red) and vertically aligned SWNTs (indicated in green).

arrays with a widely tunable average nanotube diameter. Our method can produce VA-SWNTs with an average diameter as small as 1.2 nm. This small diameter is achieved using ACCVD and catalyst particles prepared by a wet process.[6,15] Additionally, we performed a quantitative study on the diameter using a novel spectral analysis method, giving insights into the time-dependent SWNT formation process. On the basis of further investigations, a possible growth mechanism for small-diameter SWNT arrays is discussed.

RESULTS AND DISCUSSION

Characterization of VA-SWNT Morphology and Diameter. Figure 1a shows a typical SEM micrograph of a VA-SWNT array synthesized by ACCVD. The SWNTs grow perpendicular to the quartz substrate and form a self-standing forest-like array. The height of the array can be adjusted from submicrometer to hundreds of micrometers by changing CVD and catalyst preparation parameters. The average diameter of the SWNTs is approximately 2 nm using our standard procedure.[16,17] Although relatively small for vertically aligned SWNT arrays, 2 nm is considerably larger than non-aligned SWNTs synthesized by powder-supported or floating catalyst methods (*e.g.*, HiPco, CoMoCAT, and zeolite-supported ACCVD processes),[15,18,19] which yield SWNTs with diameters around 1 nm. The difference in diameter range for VA-SWNTs and random SWNT aggregates is illustrated in Figure 1b. We acknowledge that large-diameter SWNTs (2 nm or larger) may be suitable or preferable in some applications (*e.g.*, the diameter effect on device performance),[4] but small-diameter SWNTs (1 nm or less) possess considerable band gaps, clearly setting them apart from graphene for semiconductor electronics applications. The synthesis of small-diameter VA-SWNTs could advance and extend the applications of this material.

We used optical absorbance as our primary method of characterizing diameter distribution, with supplemental use of Raman scattering and TEM observations. It is important to summarize the experimental methodologies being employed to characterize SWNT diameters because the difficulty in diameter control lies not only in the synthesis protocols used but also in the characterization methods and interpretation of data. Raman spectroscopy is perhaps the most often used method because the frequency of the radial breathing mode (RBM) is directly determined by the SWNT diameter.[20] However, Raman spectra contain information from a limited number of SWNTs in the sample because excitation of the RBM is a resonance process, leaving the actual diameter distribution of bulk SWNTs unclear (unless a wide range of excitation energies are used). Furthermore, the strong dependence of Raman intensity on diameter and chirality hinders the use of this technique for the accurate estimation of diameter distribution.[21] Photoluminescence excitation spectroscopy (PLE) has more recently proved to be a powerful technique for the unambiguous identification of SWNT chiralities.[22] However, the main shortcoming of PLE is that only isolated, small-diameter, semiconducting SWNTs can be detected. Selectivity during sample preparation, a narrow detection window, and chirality-dependent quantum efficiencies also restrict the use of PLE for obtaining a statistically accurate result representative of the entire nanotube ensemble.[23,24] TEM and atomic force microscopy (AFM) in this sense are the most reliable methods, despite the complicated sample preparation and time-consuming measurement. Other strategies such as Rayleigh scattering are applicable to only well-isolated and suspended samples.[25]

Effects of CVD Parameters. Figure 2 presents resonance Raman and optical absorbance spectra of vertically aligned SWNT films grown at various CVD temperatures and pressures using our standard catalyst recipe.[6] The resonance Raman spectra were taken directly from the top of the samples with 488 nm laser excitation, and the optical absorbance spectra were obtained by titling the as-grown array 30° with respect to the Poynting vector of the incident light. Clear differences appear in the RBM region of the Raman spectra (red arrows in Figure 2a), suggesting that

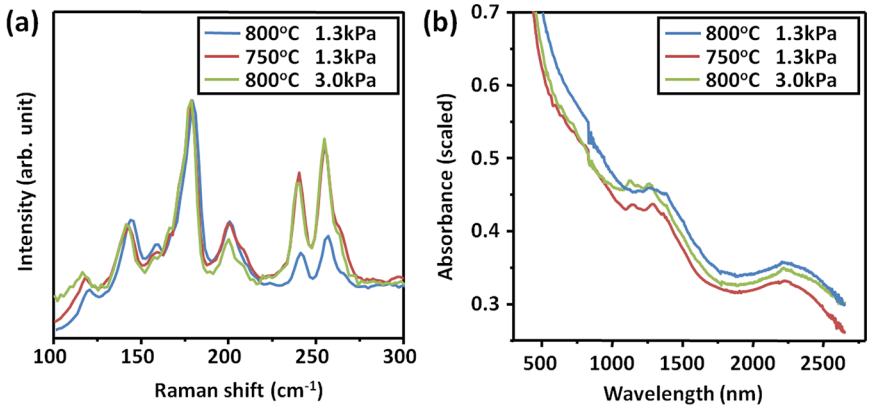

Figure 2. (a) Resonance Raman and (b) UV–Vis–NIR optical absorbance spectra of aligned SWNTs grown at different temperatures and pressures clearly show different Raman RBM peak intensities but similar absorption peak positions. Excitation wavelength in (a) was 488 nm.

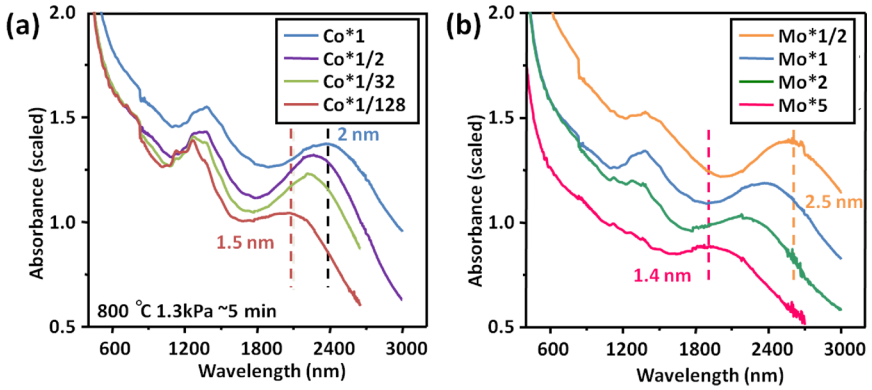

Figure 3. (a) UV–Vis–NIR optical absorbance spectra of aligned SWNTs synthesized using different catalyst recipes. The concentration of the catalyst solution is normalized by a standard value of 0.01 wt % for each of the metal species in cobalt acetate and molybdenum acetate.

SWNTs with smaller diameters are synthesized at elevated pressure and reduced temperature. The nearly identical positions of the E_{11} and E_{22} peaks in the optical absorbance (Figure 2b),[26] however, imply that the increase in the population of a minority of small-diameter SWNTs indicated by the Raman spectra is insufficient to alter the overall diameter distribution. This superficially contradictory result is because most of the strong RBM signals (145, 181, 244, 256 cm^{-1}) are from a minority population of small-diameter SWNTs randomly suspended in the forest.[27] For example, from the Kataura plot, we know that RBM peaks at 244 and 256 cm^{-1} correspond to (7,7) and (8,5) SWNTs with diameters of 0.96 and 0.90 nm,[28] which are both far from the mean diameter of VA-SWNTs. In general, due to differences in resonance conditions as well as a stronger Raman response from small-diameter near-zigzag SWNTs,[21] small differences in sample populations can be greatly exaggerated in resonance Raman spectra. This is evidenced by a careful TEM characterization in which little difference in diameter distribution is observed (not shown).

Effect of Catalyst Recipe. We find the influence of catalyst recipe on the diameters of produced SWNTs to be more significant than synthesis temperature or pressure. We have shown that the reduction of mean diameter can be achieved by modifying the reduction condition.[29] By carefully adjusting the catalyst reduction condition to inhibit aggregation of catalysts, we have obtained a mean diameter of 1.6 nm. Even though SWNTs with much smaller diameters can be obtained by exposing the catalyst to water vapor prior to CVD, vertically aligned morphology was lost due to less efficient growth from such catalysts.[29]

Since we use a bimetal Co–Mo catalyst in the present study, the effects of the two components were investigated independently. When the absolute amount of Co is decreased in the solution catalyst precursor, a clear blue shift of the E_{11} and E_{22} peaks is seen in optical absorbance (Figure 3a). Assuming the peak positions denote the mean diameter of the SWNTs inside the array, this suggests that the diameter reduces from 2 to 1.6 nm when the Co concentration is decreased by 2 orders of magnitude. This overall tendency is consistent with combinatorial experiments, in which the nominal thickness of Co and Mo were continuously changed.[13] Still, it is surprising that VA-SWNT morphology is obtained in this wide range of Co concentrations.

It seems qualitatively straightforward that a smaller amount of catalyst generates smaller catalyst particles, which produce thinner SWNTs.[30] It has also been proved that Co is the active site driving nanotube growth in our Co–Mo system.[31] However, unlike on porous catalyst supports such as zeolites, where nano-sized pores restrict the size of the catalyst,[32] nanoparticles on a flat substrate always have a temperature-dependent minimum size limit determined by the energy of the system. Furthermore, small particles can easily migrate and aggregate at elevated temperature. One common strategy to inhibit this aggregation is to introduce a secondary species, such as alumina or molybdenum.[10,13,31] Therefore, the role of Mo in our Co–Mo system is also studied independently.

Figure 3b shows optical absorbance spectra of VA-SWNTs grown using different Mo concentrations while keeping the Co concentration constant. The E_{11} and E_{22} peaks of the produced SWNTs exhibit more significant shifts than in the reduced Co case, indicating the average diameter changed from 2.5 to 1.4 nm. This diameter reduction was achieved by increasing the Mo concentration by only 10 times yet is much more significant than the reduction obtained by reducing the Co concentration by a factor of more than 100. This agrees well with the hypothesis that Mo forms an oxide (MoO_x or $CoMoO_y$) that strongly interacts with Co, thereby reducing the mobility of Co nanoparticles at high temperatures.[13,31]

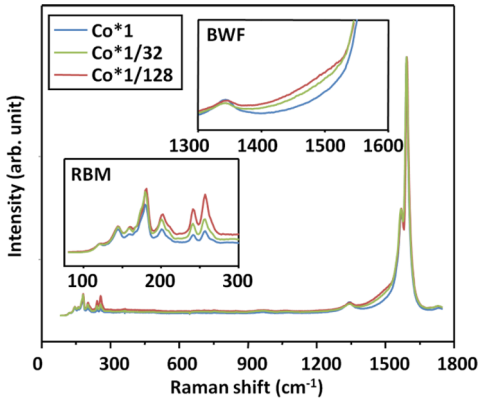

Figure 4. Resonance Raman spectra of vertically aligned SWNTs obtained from ACCVD with reduced Co amount on quartz substrates. Indication of the existence of smaller diameter SWNTs is consistent with optical absorbance spectra. Excitation wavelength was 488 nm.

Two significant changes can be observed in resonant Raman spectra (Figure 4) from the reduced-concentration-Co recipe and are consistent with the above absorption results. First, higher-frequency peaks in the RBM range are enhanced in the sample grown using the least amount of Co. This indicates an increased population of small-diameter SWNTs. Second, decreasing the amount of Co also leads to an emergence of a more intense Breit–Wigner–Fano (BWF) feature in the G-band region, also indicating an increased contribution of small-diameter metallic nanotubes such as (7,7) and (8,5). However, the relatively weak BWF signal from our VA-SWNTs for a wide range of diameters and different excitation energies (not shown) cannot be straightforwardly understood. Because a considerable contribution to the G-band from majority larger diameter and vertically aligned nanotubes is apparent from polarized Raman measurements,[27] silence of metallic nanotube features may imply that the percentage of semiconductor nanotubes is high. Similar results were obtained for the increased Mo case. As stated above, such changes in the Raman spectra are not sufficient evidence for overall diameter modulation, and agreement with absorbance spectra is necessary.

High-resolution TEM (HR-TEM) characterization was performed on samples obtained in the above-mentioned experiments. For consistency, we chose the upper portions of the arrays for all TEM observations. Micrographs of a typical SWNT array and a small-diameter array are shown in Figure 5a,b, respectively. We measured the diameters of approximately 400 SWNTs and present the statistics in Figure 5c. The histograms show three representative samples, with

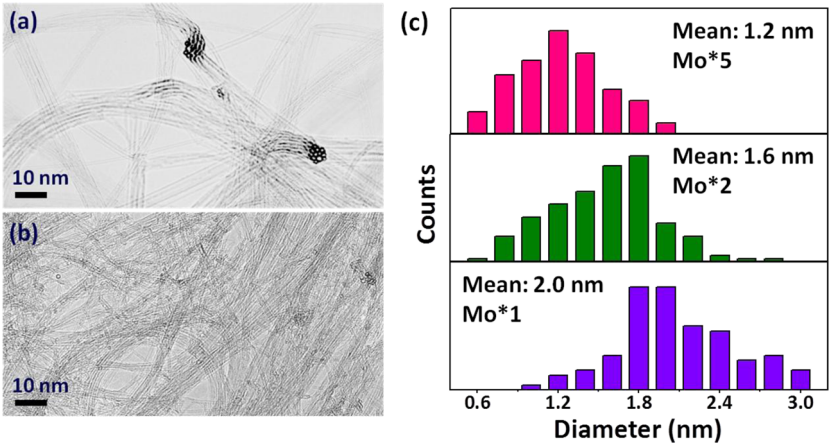

Figure 5. (a,b) Representative TEM images and (c) diameter histograms of vertically aligned SWNTs synthesized using different catalyst recipes.

average diameters of 2.0, 1.6, and 1.2 nm. Although time-consuming, this TEM measurement unambiguously reveals that the diameter distribution was successfully modulated over a broad range. Furthermore, for the d_{avg} = 1.2 nm sample, all SWNTs in the array were found to be thinner than 2 nm, which may be critically important for some applications. We note that the mean diameter estimated from optical absorbance spectra is slightly larger than the value obtained from TEM observations (*i.e.*, 1.4 nm *vs* 1.2 nm). The reason for this is explained in the following section. It is also worth noting that although SWNTs with mean diameters of less than 1.2 nm may be obtained by further reducing the Co or increasing the Mo concentration, the catalyst activity decreases dramatically and the vertical alignment is therefore lost. Very recently, we also reported the growth of nitrogen-doped VA-SWNTs with a mean diameter of less than 1 nm by using mixed ethanol/acetonitrile carbon source.[33] However, for undoped VA-SWNTs, further reducing the diameter while maintaining vertical alignment still presents a challenge.

Our present understanding of how SWNT diameter changes as a function of Mo concentration is described as follows. Co acetate decomposes during thermal annealing, and the Co then aggregates into metallic particles that act as nucleation centers for SWNT growth. The Mo species, however, forms a MoO_x or $CoMoO_y$ phase that serves to stabilize the Co metal. Since Mo is known to be much less mobile than Co at high temperature, it is rational to expect that more Mo on the substrate could better inhibit surface diffusion of Co. Therefore, the chance for Co to remain as small particles increases with added Mo. In this sense, we speculate that a similar strategy to reduce SWNT diameter may also apply to physically deposited Co/Mo films. One other point that needs to be taken into account is that Mo oxides such as MoO_3 easily evaporate at temperatures above 600 °C. However, we use Ar/H_2 as a carrier gas during the entire heating process. MoO_3 can be reduced above 400 °C, which means that although some Mo may be lost due to evaporation, a significant could remain as MoO_x or $CoMoO_y$. Our previous study revealed that the atomic concentration of Mo did decrease after reduction, but half of the material remained on the substrate.[31]

Quantitative Measurement of Diameter along the SWNT Array. Vertically aligned CNTs normally obey a root growth mechanism,[34−38] and all CNTs grow in generally the same direction. The resulting alignment enables easy access to regions in the array where CNTs formed at different times during synthesis, thus study of the time-dependent growth process becomes possible. For example, in the SEM image shown in Figure 1a, it appears that the upper portion of the array (grown earlier) is better aligned than the root (grown later). The bundle size also appears to decrease with CVD time. Resonance Raman spectra taken from different points along the cross section of the array (Figure 6a) also show a marked difference. Note that the anomalous effect of suspended nanotubes is less pronounced for excitation with a 633 nm laser.[27,39] Low-energy RBM peaks (*i.e.*, from large-diameter SWNTs) are enhanced in spectra obtained near the root of the array.

For a more quantitative characterization, we synthesized three VA-SWNT arrays (called A, B, and C for convenience) by changing only the CVD time; other parameters were kept strictly identical. The dependence of film thickness on growth time, depicted by a growth curve,[40] is shown for each array in Figure 6b. These three growth curves suggest that all three samples exhibited almost exactly the same growth behavior, having nearly identical growth rates and catalyst deactivation times. Optical absorbance spectra corresponding to each of these arrays are shown in Figure 6c, and little difference is seen in the E_{11} and E_{22} peak positions.

Assuming the only difference in these SWNT arrays is their height, we can consider the arrays are nearly approximated as combinations of the others. In this approach, array A is simply an array with a height of 3 μm and is represented by the green box in Figure 6b. Array B (height = 6 μm, purple box in Figure 6b) may be considered as two 3 μm arrays stacked on top of each other. The upper 3 μm array should be identical to array A, so subtracting spectrum A from the spectrum of array B should yield the absorbance contribution from the bottom half of array B (blue box in Figure 6b). Similarly, subtracting spectrum B from that for C gives the net absorbance of the root part of array C (red box in Figure 6b). Using this strategy, the absorbance of array C (an 8 μm SWNT array) can be decomposed into three spectra, spectrum A (top), spectrum B−A (middle), and spectrum C−B (root). The spectra decomposed in this manner are shown in Figure 6d. The peak positions are clearly different, indicating that the SWNT diameters are *not* uniform along the array, and the SWNTs synthesized last (near the root) have larger diameters than those which form first (at the top). This gradual increase of the SWNT diameter with growth time was observed before by Hasegawa *et al.* for sputtered Fe/Al catalyst but generally difficult to characterize by conventional approaches.[41] Our "sliced" optical absorbance method offers a quantitative evaluation and confirms the diameter change is approximately 20% in the present case. This diameter widening may commonly occur in various systems and thus remains a challenge for the nanotube synthesis community.

The spectra shown in Figure 6 also help to understand why the average diameter obtained from TEM is slightly smaller than suggested by optical absorbance. The difference between diameter estimates based on

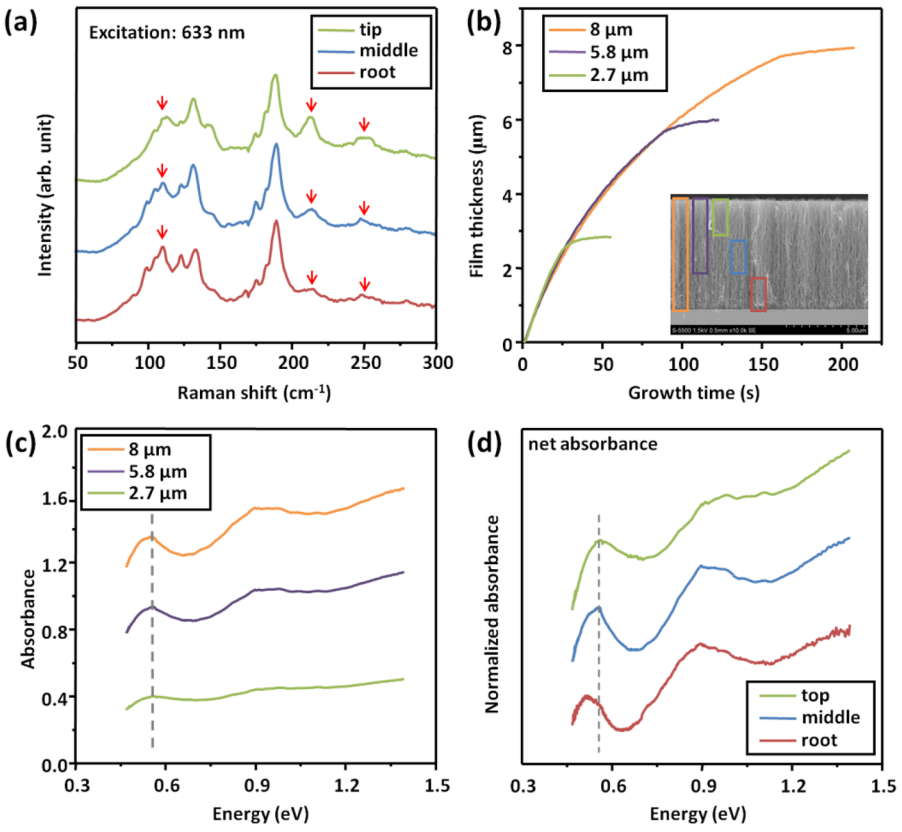

Figure 6. (a) Raman spectra obtained from the top, middle, and root of a cross section of a typical aligned SWNT array showing that the diameter of SWNTs at the root seems to be larger than at the top. Excitation wavelength was 633 nm. (b) Growth curves of three arrays grown under strictly identical CVD conditions but for different times. Inset shows the morphology of the VA-SWNTs. (c) Optical absorbance of the three arrays. (d) Net/absolute absorbance of the different parts of the 8 μm array obtained by subtracting the data in (c). Shifts in peak positions quantitatively show the diameter change occurring during synthesis.

optical absorbance and HR-TEM measurements shown in Figure 5 is likely because the former averages the entire array, whereas the latter is only representative of a local region that may not necessarily be representative of the entire array. Nevertheless, the results shown in Figure 5 indicate that VA-SWNTs with diameters as small as 1.2 nm can be obtained. Previous VA-SWNTs grown on physical vapor deposited catalyst usually have diameters larger than 2 nm.

Mechanism for Diameter Change: Ripening or Aggregation. Since the SWNT diameter is essentially determined by the size of the catalyst particle,[14] the observed diameter change reveals the behavior of the catalyst on a flat substrate. At high temperature, there are two competing mechanisms that can lead to particle growth. At CVD temperatures, the catalyst particles are mobile on the substrate and may collide with each other, forming a larger particle. Less mobile particles can also grow *via* Ostwald ripening.[41,42] The main difference between these two processes is that in Ostwald ripening small particles gradually lose atoms to larger particles, causing the larger particles to grow and smaller ones to shrink. This would cause the distribution of an ensemble of particles to shift from Gaussian to bimodal. Since our sliced absorbance spectra in Figure 6d reveal a general shift in one direction (no split in the small diameter range), it appears that catalyst aggregation—rather than Ostwald ripening—dominates catalyst behavior during the growth of our SWNTs.[43]

To confirm this speculation, we investigated the catalyst morphology by TEM after different CVD times (Supporting Information). To make the observation less challenging, we intentionally used a high-concentration catalyst solution to form slightly larger catalyst particles. TEM micrographs and a statistical histogram showing catalyst sizes (Figure S1) reveal that in the early stage of the CVD process all particles are below 3 nm, whereas after 10 min, all catalyst sizes increase to approximately 3.5 nm. No noticeable enhancement of small diameter particles was observed. These findings indicate that Ostwald ripening is not the primary mechanism behind catalyst growth in this process.

SUMMARY

We present a comprehensive study on the diameter modulation of vertically aligned SWNT arrays and show that the catalyst recipe has a much more significant impact on mean diameter than either CVD temperature or pressure. By changing both the relative and

absolute amounts of Co and Mo in a binary catalyst system, we were able to tune the average SWNT diameter between 1.2 and 2.5 nm, as determined by optical absorbance, resonance Raman spectroscopy, and HR-TEM. For the mean diameter of 1.2 nm, all of the SWNTs were found to be thinner than 2 nm. Due to their nearly doubled band gap and improved structural stiffness, such small-diameter VA-SWNTs may be desirable for optical and electronic applications. We also propose a method by which optical absorbance spectra can be decomposed to reveal contributions from different parts of an SWNT array. By this method, we reveal a 20% increase in SWNT diameter during CVD synthesis, which we attribute to catalyst aggregation rather than Ostwald ripening. These insights into the growth mechanism may help researchers to further control the synthesis of this material.

EXPERIMENTAL SECTION

Vertically aligned SWNT arrays were synthesized using ethanol as the carbon source. Co/Mo catalyst is directly prepared on the quartz substrate by dip-coating without the use of an additional support layer. The growth temperature, ethanol pressure, and concentration of the catalyst precursor were changed independently to investigate their effects on the diameter of obtained SWNTs. CVD duration was 5 min, and the ethanol flow was 450 sccm in all cases. Additional details about the catalyst preparation and CVD procedure may be found in our previous reports.[6,44] The as-grown SWNT array was characterized by scanning electron microscopy (SEM, Hitachi-5500), resonance Raman spectroscopy (488 and 633 nm excitation wavelengths), UV−Vis−NIR absorbance spectroscopy (Shimadzu UV-3150), and transmission electron microscopy (TEM, JEOL 2000EXII operated at 120 kV).

Conflict of Interest: The authors declare no competing financial interest.

Acknowledgment. Part of this work was financially supported by Grant-in-Aid for Scientific Research (22226006, 19054003, 23760179, and 23760180), JSPS Core-to-Core Program, the "Global Center for Excellence for Mechanical Systems Innovation" program at the University of Tokyo, National Science Foundation of China (51002190), and Guangdong Provincial Natural Science Foundation of China.

Supporting Information Available: Typical TEM images and diameter distribution histogram of the catalyst particles at the root of an SWNT array after 10 min CVD. This material is available free of charge *via* the Internet at http://pubs.acs.org.

REFERENCES AND NOTES

1. Burda, C.; Chen, X. B.; Narayanan, R.; El-Sayed, M. A. Chemistry and Properties of Nanocrystals of Different Shapes. *Chem. Rev.* **2005**, *105*, 1025–1102.
2. Hu, J. T.; Odom, T. W.; Lieber, C. M. Chemistry and Physics in One Dimension: Synthesis and Properties of Nanowires and Nanotubes. *Acc. Chem. Res.* **1999**, *32*, 435–445.
3. Jiao, L. Y.; Zhang, L.; Wang, X. R.; Diankov, G.; Dai, H. J. Narrow Graphene Nanoribbons from Carbon Nanotubes. *Nature* **2009**, *458*, 877–880.
4. Asada, Y.; Nihey, F.; Ohmori, S.; Shinohara, H.; Saito, T. Diameter-Dependent Performance of Single-Walled Carbon Nanotube Thin-Film Transistors. *Adv. Mater.* **2011**, *23*, 4631–4635.
5. Kataura, H.; Kumazawa, Y.; Maniwa, Y.; Umezu, I.; Suzuki, S.; Ohtsuka, Y.; Achiba, Y. Optical Properties of Single-Wall Carbon Nanotubes. *Synth. Met.* **1999**, *103*, 2555–2558.
6. Murakami, Y.; Chiashi, S.; Miyauchi, Y.; Hu, M. H.; Ogura, M.; Okubo, T.; Maruyama, S. Growth of Vertically Aligned Single-Walled Carbon Nanotube Films on Quartz Substrates and Their Optical Anisotropy. *Chem. Phys. Lett.* **2004**, *385*, 298–303.
7. Yamada, T.; Namai, T.; Hata, K.; Futaba, D. N.; Mizuno, K.; Fan, J.; Yudasaka, M.; Yumura, M.; Iijima, S. Size-Selective Growth of Double-Walled Carbon Nanotube Forests from Engineered Iron Catalysts. *Nat. Nanotechnol.* **2006**, *1*, 131–136.
8. Nessim, G. D.; Hart, A. J.; Kim, J. S.; Acquaviva, D.; Oh, J. H.; Morgan, C. D.; Seita, M.; Leib, J. S.; Thompson, C. V. Tuning of Vertically-Aligned Carbon Nanotube Diameter and Areal Density through Catalyst Pre-treatment. *Nano Lett.* **2008**, *8*, 3587–3593.
9. Zhong, G. F.; Warner, J. H.; Fouquet, M.; Robertson, A. W.; Chen, B. A.; Robertson, J. Growth of Ultrahigh Density Single-Walled Carbon Nanotube Forests by Improved Catalyst Design. *ACS Nano* **2012**, *6*, 2893–2903.
10. Hata, K.; Futaba, D. N.; Mizuno, K.; Namai, T.; Yumura, M.; Iijima, S. Water-Assisted Highly Efficient Synthesis of Impurity-Free Single-Walled Carbon Nanotubes. *Science* **2004**, *306*, 1362–1364.
11. Zhang, G. Y.; Mann, D.; Zhang, L.; Javey, A.; Li, Y. M.; Yenilmez, E.; Wang, Q.; McVittie, J. P.; Nishi, Y.; Gibbons, J.; *et al.* Ultra-High-Yield Growth of Vertical Single-Walled Carbon Nanotubes: Hidden Roles of Hydrogen and Oxygen. *Proc. Natl. Acad. Sci. U.S.A.* **2005**, *102*, 16141–16145.
12. Zhong, G. F.; Iwasaki, T.; Honda, K.; Furukawa, Y.; Ohdomari, I.; Kawarada, H. Low Temperature Synthesis of Extremely Dense, and Vertically Aligned Single-Walled Carbon Nanotubes. *Jpn. J. Appl. Phys.* **2005**, *44*, 1558–1561.
13. Sugime, H.; Noda, S.; Maruyama, S.; Yamaguchi, Y. Multiple "Optimum" Conditions for Co−Mo Catalyzed Growth of Vertically Aligned Single-Walled Carbon Nanotube Forests. *Carbon* **2009**, *47*, 234–241.
14. Homma, Y.; Kobayashi, Y.; Ogino, T.; Takagi, D.; Ito, R.; Jung, Y. J.; Ajayan, P. M. Role of Transition Metal Catalysts in Single-Walled Carbon Nanotube Growth in Chemical Vapor Deposition. *J. Phys. Chem. B* **2003**, *107*, 12161–12164.
15. Maruyama, S.; Kojima, R.; Miyauchi, Y.; Chiashi, S.; Kohno, M. Low-Temperature Synthesis of High-Purity Single-Walled Carbon Nanotubes from Alcohol. *Chem. Phys. Lett.* **2002**, *360*, 229–234.
16. Murakami, Y.; Einarsson, E.; Edamura, T.; Maruyama, S. Polarization Dependent Optical Absorption Properties of Single-Walled Carbon Nanotubes and Methodology for the Evaluation of Their Morphology. *Carbon* **2005**, *43*, 2664–2676.
17. Xiang, R.; Yang, Z.; Zhang, Q.; Luo, G. H.; Qian, W. Z.; Wei, F.; Kadowaki, M.; Einarsson, E.; Maruyama, S. Growth Deceleration of Vertically Aligned Carbon Nanotube Arrays: Catalyst Deactivation or Feedstock Diffusion Controlled? *J. Phys. Chem. C* **2008**, *112*, 4892–4896.
18. Nikolaev, P.; Bronikowski, M. J.; Bradley, R. K.; Rohmund, F.; Colbert, D. T.; Smith, K. A.; Smalley, R. E. Gas-Phase Catalytic Growth of Single-Walled Carbon Nanotubes from Carbon Monoxide. *Chem. Phys. Lett.* **1999**, *313*, 91–97.
19. Bachilo, S. M.; Balzano, L.; Herrera, J. E.; Pompeo, F.; Resasco, D. E.; Weisman, R. B. Narrow (*n*,*m*)-Distribution of Single-Walled Carbon Nanotubes Grown Using a Solid Supported Catalyst. *J. Am. Chem. Soc.* **2003**, *125*, 11186–11187.
20. Jorio, A.; Saito, R.; Hafner, J. H.; Lieber, C. M.; Hunter, M.; McClure, T.; Dresselhaus, G.; Dresselhaus, M. S. Structural (*n*,*m*) Determination of Isolated Single-Wall Carbon Nanotubes by Resonant Raman Scattering. *Phys. Rev. Lett.* **2001**, *86*, 1118–1121.

21. Sato, K.; Saito, R.; Nugraha, A. R. T.; Maruyama, S. Excitonic Effects on Radial Breathing Mode Intensity of Single Wall Carbon Nanotubes. *Chem. Phys. Lett.* **2010**, *497*, 94–98.
22. O'Connell, M. J.; Bachilo, S. M.; Huffman, C. B.; Moore, V. C.; Strano, M. S.; Haroz, E. H.; Rialon, K. L.; Boul, P. J.; Noon, W. H.; Kittrell, C.; *et al.* Band Gap Fluorescence from Individual Single-Walled Carbon Nanotubes. *Science* **2002**, *297*, 593–596.
23. Oyama, Y.; Saito, R.; Sato, K.; Jiang, J.; Samsonidze, G. G.; Gruneis, A.; Miyauchi, Y.; Maruyama, S.; Jorio, A.; Dresselhaus, G.; *et al.* Photoluminescence Intensity of Single-Wall Carbon Nanotubes. *Carbon* **2006**, *44*, 873–879.
24. Tsyboulski, D. A.; Rocha, J. D. R.; Bachilo, S. M.; Cognet, L.; Weisman, R. B. Structure-Dependent Fluorescence Efficiencies of Individual Single-Walled Carbon Nanotubes. *Nano Lett.* **2007**, *7*, 3080–3085.
25. Sfeir, M. Y.; Wang, F.; Huang, L. M.; Chuang, C. C.; Hone, J.; O'Brien, S. P.; Heinz, T. F.; Brus, L. E. Probing Electronic Transitions in Individual Carbon Nanotubes by Rayleigh Scattering. *Science* **2004**, *306*, 1540–1543.
26. Tian, Y.; Nasibulin, A. G.; Aitchison, B.; Nikitin, T.; von Pfaer, J.; Jiang, H.; Zhu, Z.; Khriachtchev, L.; Brown, D. P.; Kauppinen, E. I. Controlled Synthesis of Single-Walled Carbon Nanotubes in an Aerosol Reactor. *J. Phys. Chem. C* **2011**, *115*, 7309–7318.
27. Zhang, Z. Y.; Einarsson, E.; Murakami, Y.; Miyauchi, Y.; Maruyama, S. Polarization Dependence of Radial Breathing Mode Peaks in Resonant Raman Spectra of Vertically Aligned Single-Walled Carbon Nanotubes. *Phys. Rev. B* **2010**, *81*, 165442-1-9.
28. Araujo, P. T.; Doorn, S. K.; Kilina, S.; Tretiak, S.; Einarsson, E.; Maruyama, S.; Chacham, H.; Pimenta, M. A.; Jorio, A. Third and Fourth Optical Transitions in Semiconducting Carbon Nanotubes. *Phys. Rev. Lett.* **2007**, *98*, 067401-1-4.
29. Thurakitseree, T.; Einarsson, E.; Xiang, R.; Zhao, P.; Aikawa, S.; Chiashi, S.; Shiomi, J.; Maruyama, S. Diameter Controlled Chemical Vapor Deposition Synthesis of Single-Walled Carbon Nanotubes. *J. Nanosci. Nanotechnol.* **2012**, *12*, 370–376.
30. Helveg, S.; Lopez-Cartes, C.; Sehested, J.; Hansen, P. L.; Clausen, B. S.; Rostrup-Nielsen, J. R.; Abild-Pedersen, F.; Norskov, J. K. Atomic-Scale Imaging of Carbon Nanofibre Growth. *Nature* **2004**, *427*, 426–429.
31. Hu, M. H.; Murakami, Y.; Ogura, M.; Maruyama, S.; Okubo, T. Morphology and Chemical State of Co−Mo Catalysts for Growth of Single-Walled Carbon Nanotubes Vertically Aligned on Quartz Substrates. *J. Catal.* **2004**, *225*, 230–239.
32. Okamoto, A.; Shinohara, H. Control of Diameter Distribution of Single-Walled Carbon Nanotubes Using the Zeolite-CCVD Method at Atmospheric Pressure. *Carbon* **2005**, *43*, 431–436.
33. Thurakitseree, T.; Kramberger, C.; Zhao, P.; Aikawa, S.; Harish, S.; Chiashi, S.; Einarsson, E.; Maruyama, S. Diameter-Controlled and Nitrogen-Doped Vertically Aligned Single-Walled Carbon Nanotubes. *Carbon* **2012**, *50*, 2635–2640.
34. Liu, L.; Fan, S. S. Isotope Labeling of Carbon Nanotubes and Formation of $^{12}C-^{13}C$ Nanotube Junctions. *J. Am. Chem. Soc.* **2001**, *123*, 11502–11503.
35. Li, X.; Cao, A. Y.; Jung, Y. J.; Vjatai, R.; Ajayan, P. M. Bottom-Up Growth of Carbon Nanotube Multilayers: Unprecedented Growth. *Nano Lett.* **2005**, *5*, 1997–2000.
36. Xiang, R.; Luo, G. H.; Qian, W. Z.; Zhang, Q.; Wang, Y.; Wei, F.; Li, Q.; Cao, A. Y. Encapsulation, Compensation, and Substitution of Catalyst Particles during Continuous Growth of Carbon Nanotubes. *Adv. Mater.* **2007**, *19*, 2360–2360.
37. Xiang, R.; Zhang, Z.; Ogura, K.; Okawa, J.; Einarsson, E.; Miyauchi, Y.; Shiomi, J.; Maruyama, S. Vertically Aligned ^{13}C Single-Walled Carbon Nanotubes from No-Flow Alcohol Chemical Vapor Deposition and Their Root Growth Mechanism. *Jpn. J. Appl. Phys.* **2008**, *47*, 1971–1974.
38. Iwasaki, T.; Zhong, G. F.; Aikawa, T.; Yoshida, T.; Kawarada, H. Direct Evidence for Root Growth of Vertically Aligned Single-Walled Carbon Nanotubes by Microwave Plasma Chemical Vapor Deposition. *J. Phys. Chem. B* **2005**, *109*, 19556–19559.
39. Murakami, Y.; Chiashi, S.; Einarsson, E.; Maruyama, S. Polarization Dependence of Resonant Raman Scattering from Vertically Aligned Single-Walled Carbon Nanotube Films. *Phys. Rev. B* **2005**, *71*, 085403-1-8.
40. Einarsson, E.; Murakami, Y.; Kadowaki, M.; Maruyama, S. Growth Dynamics of Vertically Aligned Single-Walled Carbon Nanotubes from *In Situ* Measurements. *Carbon* **2008**, *46*, 923–930.
41. Hasegawa, K.; Noda, S. Millimeter-Tall Single-Walled Carbon Nanotubes Rapidly Grown with and without Water. *ACS Nano* **2011**, *5*, 975–984.
42. Hasegawa, K.; Noda, S. Moderating Carbon Supply and Suppressing Ostwald Ripening of Catalyst Particles to Produce 4.5-mm-Tall Single-Walled Carbon Nanotube Forests. *Carbon* **2011**, *49*, 4497–4504.
43. Sakurai, S.; Nishino, H.; Futaba, D.; Yasuda, S.; Yamada, T.; Maigne, A.; Matsuo, Y.; Nakamura, E.; Yumura, M.; Hata, K. Role of Subsurface Diffusion and Ostwald Ripening in Catalyst Formation for Single-Walled Carbon Nanotube Forest Growth. *J. Am. Chem. Soc.* **2012**, *134*, 2148–2153.
44. Xiang, R.; Wu, T. Z.; Einarsson, E.; Suzuki, Y.; Murakami, Y.; Shiomi, J.; Maruyama, S. High-Precision Selective Deposition of Catalyst for Facile Localized Growth of Single-Walled Carbon Nanotubes. *J. Am. Chem. Soc.* **2009**, *131*, 10344–10345.